Modeling of VSC-Based Power Systems in the Extended Harmonic Domain

Miguel Esparza, *Student Member, IEEE*, Juan Segundo-Ramírez, *Member, IEEE*,
Jun Bum Kwon, *Student Member, IEEE*, Xiongfei Wang, *Member, IEEE*, and Frede Blaabjerg, *Fellow, IEEE*

***Abstract*—Averaged modeling is a commonly used approach used to obtain mathematical representations of VSC-based systems. However, essential characteristics mainly related to the modulation process and the harmonic distortion of the signals are not able to be accurately captured and analyzed. The extended harmonic domain (EHD) has recently been seen as an alternative modeling framework since it allows us to consider the harmonic interaction explicitly. However, there is not a clearly established methodology to derive the EHD models in the presence of power electronic switches. This paper presents a generalized methodology based on the switching instants to obtain large-signal EHD models of VSC-based power systems. Three model order reduction approaches are also proposed to address the increased size of the resulting EHD models. Analytic formulas of three modulation techniques: sinusoidal pulse-width modulation, third harmonic injection pulse-width modulation, and space vector pulse-width modulation are provided to obtain the open-loop large signal EHD models. A performance assessment of the proposed modeling approach in respect to model size, the computational time and the accuracy is presented based on simulations and experimental case studies. The obtained results show that the resulting EHD models are accurate and reliable, while the memory and computation time are improved with the proposed model order reductions.**

***Index Terms*—Harmonics, modeling, sinusoidal pulse-width modulation (SPWM), space vector pulse-width modulation (SVPWM), third harmonic injection pulse-width modulation (THPWM), voltage source converter.**

I. Introduction

NEW trends in grid integration of renewable energy sources, such as distributed generations, microgrids, and large scale renewable power plants, foster the development of voltage source converters (VSC) based technologies in power systems [1]–[3]. The interconnected VSC-based applications has brought challenges, mainly associated with harmonic interaction problems [4]–[8]. To deal with these problems, detailed mathematical models for steady-state and transient analysis have to be developed and properly used.

The difficulties in the modeling of the switching-based devices, like the VSC-based systems, are due to their nonlinear and discontinuous nature of their power switches. The switched systems can be understood as a family of continuous dynamical subsystems, where an active subsystem at every time interval is selected based on commutation rules [9]. The interaction and effects of commutating among subsystems are complex, since the dynamics of the commutations are nonlinear and could be at very high frequencies.

Averaged modeling has been widely used for power electronic systems since it allows the transformation of these discrete time-varying systems into continuous time-invariant systems. In this way, the prevailing theory developed for continuous time-invariant systems can be applied in their analysis and control [10]–[12]. The increasing penetration of power electronic converters along with the increased power and voltage ratings brought new challenges in respect to harmonic interaction with power systems under both, steady-state and transient conditions [5], [13], power quality standards compliance [14], stability issues [4], [7], [8], among others. Although averaged modeling has been widely used to address these challenges, mathematical models that explicitly consider the harmonic interaction between the interconnected switched systems are more suitable to deal with them [15]–[17]. Examples of those are: dynamic phasor modeling [18], dynamic state space modeling [19], time-frequency modeling [20], extended harmonic domain (EHD) modeling [21], also known as harmonic state space (HSS) [22], and dynamic harmonic domain [23] modeling.

The EHD was proposed a decade for the analysis of power systems in order to explicitly consider the harmonics in harmonic distorted systems using a continuous dynamical model [21]. Recently, this modeling approach was used in the power electronics systems to address emerging issues such as interactions between the paralleled converters [24], [25], the effect of voltage distortion at the switching instants of power converters [26], steady-state analysis and design of passive components [3], harmonic impact on the converter controller stability [25], optimal design [27], and design of VSC-based microgrids [28].

However the derivation of EHD models for power electronics systems is not a trivial task. Some proposals have been reported [29], in which the open-loop and closed-loop models of power electronic systems are addressed. These models

Manuscript received August 5, 2016; revised October 25, 2016 and December 15, 2016; accepted January 22, 2017. Date of publication January 25, 2017; date of current version March 24, 2017. Recommended for publication by Associate Editor Y. Xue.

M. Esparza and J. Segundo-Ramírez are with the Facultad de Ingenieria, Universidad Autonoma de San Luis Potosi, San Luis Potosi 78290, Mexico (e-mail: miesparza@hotmail.com; juan.segundo@uaslp.mx).

J. B. Kwon, X. Wang, and F. Blaabjerg are with the Department of Energy Technology, Aalborg University, Aalborg 9220, Denmark (e-mail: jbk@et.aau.dk; xwa@et.aau.dk; fbl@et.aau.dk).

This paper has supplementary downloadable multimedia material available at http://ieeexplore.ieee.org provided by the authors. This material is 63.1 KB in size.

Color versions of one or more of the figures in this paper are available online at http://ieeexplore.ieee.org.

Digital Object Identifier 10.1109/TPEL.2017.2658340

are mainly based on the Fast Fourier Transform (FFT) and simulations based on the harmonic injection method. As a result, the model-order size (the number of considered harmonics) is limited by the complexity and time consumption of the modeling methodology. These methodologies do not show intuitive relation between the EHD models and the corresponding switched models in the time domain, which could be directly implied when proper functions are provided. Despite the great potential offered by this modeling approach, shown by recently reported applications, their usage for power electronic systems has been limited due to the complexity for deriving and treating EHD models which considers the switching harmonics.

In order to facilitate the use of the EHD modeling approach for power electronics systems, this paper presents a generic, yet easy-to-implement methodology to obtain the open-loop large signal EHD models of VSC-based power systems. This proposal is based on the switching instants calculation of the mostly used PWM techniques. Analytic formulas for Sinusoidal-PWM (SPWM), third Harmonic injection PWM (THPWM), and Space Vector PWM (SVPWM) techniques are proposed and provided as MATLAB functions in order to be transparently used. Three simplification approaches to the obtained models are also proposed to address the increased size of the resulting EHD models. Those are based on well-known three-phase balance relationships and the steady-state calculation obtained from the EHD steady-state model. The proposed simplifications permit to obtain accurate reduced-order EHD models for high switching frequency converters. The model size, computational burden, and model accuracy are compared among the proposed simplified models, for which an experimental validation is also presented. The obtained results show that the proposed modeling methodology leads to efficient, yet adequate EHD models, while the memory and computation burdens are appropriately addressed.

The paper is organized as follows. Section II presents the EHD model fundamentals focusing on VSC-based systems. Section III presents an universal LCL-VSC converter case study, where the periodic switched time-domain model and the PWM switching-instant-based model are used as the basis for developing the EHD model. In Section IV, the EHD model is derived based on the time-domain models of previous section. Section V presents the simplification methods for the derived EHD models. Simulation and experimental validations along with a discussion of the benefits offered by the EHD modeling are provided in Section VI. Finally, the concluding remarks are given in Section VII.

II. EHD Modeling

A. Dynamic Model

The EHD is a reference frame that allows the modeling of electric power networks in steady state and transient state. From the complex Fourier series, any periodic signal can be expressed as

$$x(t) = \sum_{k=-\infty}^{\infty} X_{\langle k\rangle} e^{jk\omega_0 t} \tag{1}$$

where $\omega_0 = 2\pi/T_0$ is the angular fundamental frequency of period T_0. $X_{\langle k\rangle}$ is the kth complex Fourier series coefficient of $x(t)$, given by

$$X_{\langle k\rangle} = \frac{1}{T_0}\int_{t-T_0}^{t} x(t)e^{-jk\omega_0 t}dt. \tag{2}$$

A realizable representation of (1) is obtained if the limit of its summation is a finite number h, which determines the maximum harmonic order considered. In this way, the discrete nature of certain signals (such as the switching signals of power switches) can be treated as continuous by considering its finite complex Fourier series representation. In this way any signal can be conveniently expressed by

$$x(t) = \mathcal{G}(t)\mathbf{X}(t) \tag{3}$$

where the vector $\mathbf{G}(t)$ is the time-dependent orthogonal basis of the Fourier series defined by

$$\mathcal{G}(t) = \left[e^{-jh\omega_0 t}, \dots, e^{-j\omega_0 t}, 1, e^{j\omega_0 t}, \dots, e^{jh\omega_0 t}\right] \tag{4}$$

and $\mathbf{X}(t)$ is a complex vector that contains the time-varying complex Fourier series coefficients

$$\begin{aligned}\mathbf{X}(t) = [&X_{\langle -h\rangle}(t), \dots, X_{\langle -1\rangle}(t), X_{\langle 0\rangle}(t),\\ &X_{\langle 1\rangle}(t), \dots, X_{\langle h\rangle}(t)]^T.\end{aligned} \tag{5}$$

In order to obtain the description of the generic time-variant model in the EHD, two important operations has to be described: the derivative of (3), $\frac{d}{dt}x(t)$, and its multiplication with a periodic function, $a(t)x(t)$. The derivative, $\frac{d}{dt}x(t)$ is given by

$$\frac{d}{dt}x(t) = \dot{\mathcal{G}}(t)\mathbf{X}(t) + \mathcal{G}(t)\dot{\mathbf{X}}(t) \tag{6}$$

where $\dot{\mathcal{G}}(t)$ can be conveniently described by

$$\dot{\mathcal{G}}(t) = \mathcal{G}(t)\mathbf{D} \tag{7}$$

with $\mathbf{D}$ as the EHD derivative matrix defined by

$$\mathbf{D} = \text{diag}\left(-jh\omega_0, \dots, -j\omega_0, 0, j\omega_0, \dots, jh\omega_0\right). \tag{8}$$

Hence, (6) is rewritten as

$$\frac{d}{dt}x(t) = \mathcal{G}(t)\left(\mathbf{D}\mathbf{X}(t) + \dot{\mathbf{X}}(t)\right). \tag{9}$$

The product of a periodic function $a(t)$ with $x(t)$ is expressed in the EHD, as

$$a(t)x(t) = \mathcal{G}(t)[\mathbf{A}]\mathbf{X}(t) \tag{10}$$

where $[\mathbf{A}]$ has a Toeplitz structure, which is formed with the complex Fourier series coefficients of $a(t)$, arranged in the

following form:

$$[\mathbf{A}] = \begin{bmatrix} A_{\langle 0\rangle} & A_{\langle -1\rangle} & \dots & A_{\langle -h\rangle} & & & \\ A_{\langle 1\rangle} & \ddots & \ddots & \ddots & \ddots & & \\ \vdots & \ddots & A_{\langle 0\rangle} & A_{\langle -1\rangle} & \ddots & \ddots & \\ A_{\langle h\rangle} & \ddots & A_{\langle 1\rangle} & A_{\langle 0\rangle} & A_{\langle -1\rangle} & \ddots & A_{\langle -h\rangle} \\ & \ddots & \ddots & A_{\langle 1\rangle} & A_{\langle 0\rangle} & \ddots & \vdots \\ & & \ddots & \ddots & \ddots & \ddots & A_{\langle -1\rangle} \\ & & & A_{\langle h\rangle} & \dots & A_{\langle 1\rangle} & A_{\langle 0\rangle} \end{bmatrix}. \tag{11}$$

From now on this notation (bold capital letter between square brackets) will be used to describe an EHD variable as expressed in (11). A direct implication of (10) is the multiplication by a constant $c\,x(t)$. In this case the product is given by

$$c\,x(t) = \mathcal{G}(t)[\mathbf{C}]\mathbf{X}(t) = \mathcal{G}(t)c\mathbf{I}_d\mathbf{X}(t) \tag{12}$$

where $\mathbf{I}_d$ is the identity matrix of size $(2h+1 \times 2h+1)$.

VSC-based systems are usually expressed as state-space time-domain switched models generically expressed in the form

$$\begin{aligned} \dot{x}(t) &= a(t)x(t) + b(t)u(t) \\ y(t) &= c(t)x(t) + e(t)u(t) \end{aligned} \tag{13}$$

where $x(t)$ contains the state variables; matrices $a(t)$, $b(t)$, $c(t)$, and $e(t)$ are formed from the system topology information and they include the passive parameters and switching functions; $u(t)$ and $y(t)$ contain the input and output functions, respectively. Notice that although discontinuous, by the usage of PWM to generate the switching signals, all the involved signals present a periodic steady state with a fundamental period T_0.

For a time-domain switched model, which explicitly considers the switching functions on its formulation in the form of (13), an equivalent state-space EHD representation can be written as

$$\begin{aligned} \dot{\mathbf{X}}(t) &= \mathbf{A}\mathbf{X}(t) + \mathbf{B}\mathbf{U}(t) \\ \mathbf{Y}(t) &= \mathbf{C}\mathbf{X}(t) + \mathbf{E}\mathbf{U}(t) \end{aligned} \tag{14}$$

where $\mathbf{A} = ([\mathbf{A}] - \mathbf{D})$, $\mathbf{B} = [\mathbf{B}]$, $\mathbf{C} = [\mathbf{C}]$, and $\mathbf{E} = [\mathbf{E}]$. Notice that for periodic switching signals, those are the constant state-space matrices of an LTI system.

The equation system in (14) contains the core equations of the EHD. Under this modeling domain, each time-domain state variable is replaced by $2h+1$ state equations that correspond to the harmonic contents of each time-domain state variable.

B. Steady-State Calculation

One of the key characteristic of the EHD modeling is the straightforward calculation of the steady-state solution, which is equivalent to the Harmonic Domain model of the system [30]. This can be obtained by solving the system (14), when the dynamic is zero ($\dot{\mathbf{X}} = 0$) as follows:

$$\mathbf{X}_{ss} = -\mathbf{A}^{-1}(\mathbf{B}\mathbf{U}). \tag{15}$$

From the EHD steady-state solution, many useful applications can be proposed. The direct and most common is the steady-state initial condition calculation of the system, which may be difficult to obtain in the time-domain. More advanced applications are derived from this characteristic such as the calculation of the steady-state modulation parameters, exact design of passive components and their derived analysis [3] and also doing optimal design [27], [28].

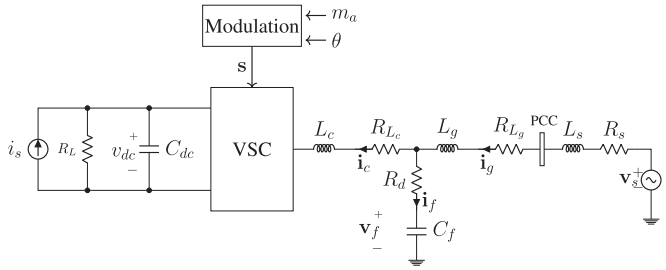

Fig. 1. LCL filter based VSC.

III. Time-Domain Switched Model of VSC-Based Systems

As stated in the previous section, one of the key features of the proposed EHD model is the direct relationship between the time-domain switched models and EHD models. The proposed EHD modeling methodology uses this relationship to directly derive EHD models from their time-domain counterparts. In order to illustrate this modeling methodology the LCL-filtered VSC shown in Fig. 1 is considered. In this schematic system the bold variables represent three-phase elements vectors, i.e., $\mathbf{i}_g = [i_{g_a}\ i_{g_b}\ i_{g_c}]^T$. The modulation block could be selected to work with three PWM-based modulation techniques: 1) SPWM, 2) THPWM, and 3) SVPWM. As a result of the modulation block, signal $\mathbf{s}$ provides the discontinuous switching functions of each leg of the converter. Notice that this is a generic system proposal, which depends on the considered parameters and can work as rectifier, inverter, or compensator.

A. Time-Domain Switched Model

The time-domain switched model from which the EHD model is derived is given by

$$\begin{aligned} \frac{d}{dt}\mathbf{i}_g &= -\frac{R_{E_g}}{L_{E_g}}\mathbf{i}_g + \frac{R_d}{L_{E_g}}\mathbf{i}_c - \frac{1}{L_{E_g}}\mathbf{v}_f + \frac{1}{L_{E_g}}\mathbf{v}_s \\ \frac{d}{dt}\mathbf{i}_c &= \frac{R_s}{L_c}\mathbf{i}_g - \frac{R_{E_c}}{L_c}\mathbf{i}_c + \frac{1}{L_c}\mathbf{v}_f - \frac{\mathbf{g}}{L_c}v_{\mathrm{dc}} \\ \frac{d}{dt}\mathbf{v}_f &= \frac{1}{C_f}\mathbf{i}_g - \frac{1}{C_f}\mathbf{i}_c \\ \frac{d}{dt}v_{\mathrm{dc}} &= \frac{\mathbf{s}}{C_{\mathrm{dc}}}\mathbf{i}_c^T - \frac{1}{R_L\,C_{\mathrm{dc}}}v_{\mathrm{dc}} + \frac{1}{C_{\mathrm{dc}}}i_s \end{aligned} \tag{16}$$

where the grid and converter equivalent resistances are given by $R_{E_g} = R_s + R_{L_g} + R_d$ and $R_{E_c} = R_d + R_{L_c}$, respectively. Similarly, the grid equivalent inductance is given by $L_{E_g} = L_s + L_g$. The switching functions contained in thee phase signal $\mathbf{s} = [s_a, s_g, s_c]^T$ are used to calculate ac to dc transfer

function of the converter, which is depicted in the model by $\mathbf{g} = [g_a, g_b, g_c]^T$ and it is given by

$$g_x = s_x - \frac{s_a + s_b + s_c}{3} \quad \text{with} \quad x = a, b, c. \tag{17}$$

Notice that the behavior of model in (16) is entirely defined by the value of the switching function $\mathbf{s}$. A complete description in both, time-domain, and EHD models, should include the source of such functions in the model. Since sinusoidal PWM techniques are the most used to generate them, the following section focus on their time-domain modeling towards the derivation of EHD models.

B. PWM-Based Switching Functions

The main basis of three phase sinusoidal PWM modulation is the comparison of a modulation signal $\mathbf{s}^{\mathrm{m}} = [s_a^{\mathrm{m}}, s_b^{\mathrm{m}}, s_c^{\mathrm{m}}]^T$ with a carrier signal $c(t)$ with a fixed switching frequency $f_{\mathrm{sw}} = m_f f_0$, where m_f is the frequency modulation index and $f_0 = 1/T_0$ is the fundamental frequency. If analytic descriptions of the carrier and the modulation signals are available, discontinuous switching functions can be described as follows:

$$s_x = \begin{cases} 1 & s_x^{\mathrm{m}} > c(t) \\ 0 & s_x^{\mathrm{m}} \leq c(t) \end{cases} \quad \text{for} \quad x = a, b, c. \tag{18}$$

Although discontinuous, (18) provides a time-domain formulation of the switching signals which explicitly considers the modulation process by means of the modulation signal. This description is valid for any modulation technique as long as a proper analytic description of its modulation signals is provided. A generic analytic description of sinusoidal PWM modulation signals is given by [31]:

$$s_x^{\mathrm{m}} = C\, m_a \sin(\omega_0 t + \theta) + e \quad \text{for} \quad x = a, b, c \tag{19}$$

where $\omega_0 = 2\pi f_0$ and the fixed parameters which determine the specific modulation technique are C as a modulation gain and e as an injected harmonics term. The input parameters that change the characteristics of the modulation signals are the modulation index $m_a \in [0, 1]$ and the phase shift $\theta \in [-\pi, \pi]$. Specifications for the three modulation techniques are given below:

1) Sinusoidal PWM: This is the basic modulation technique for which no injected harmonics are considered and no modulation gain is required. Hence, for this modulation technique $e = 0$ and $C = 1$.

2) Third Harmonic Injection PWM: In this modulation technique the modulation gain is $C = 2/\sqrt{3}$ and the injected harmonic term is given by $e = \frac{m_a}{3\sqrt{3}} \sin(3\phi)$.

3) Space Vector PWM: For this modulation technique the modulation gain is $C = 2/\sqrt{3}$ and the injected harmonics term is given by $e = -(m^*_{\max} + m^*_{\min})/2$, considering $m^*_{\max} = \max(m_a^*, m_c^*, m_c^*)$ and $m^*_{\min} = \min(m_a^*, m_c^*, m_c^*)$.

IV. EHD Modeling of a VSC-Based System

Any time-domain switched model, such as the described by (16), can be directly transformed into an EHD model by applying the derivative, periodic multiplication, and constant multiplication properties derived in (9), (10), and (12), respectively. For the presented study case system in Fig. 1, the resulting EHD domain model is given by

$$\begin{aligned}
\frac{d}{dt}\mathbf{I}_g &= \left(-\frac{R_{E_g}}{L_{E_g}}\mathbf{I}_{d_3} - \mathbf{D}_3\right)\mathbf{I}_g + \frac{R_d}{L_{E_g}}\mathbf{I}_{d_3}\mathbf{I}_c - \frac{1}{L_{E_g}}\mathbf{I}_{d_3}\mathbf{V}_f \\
&\quad + \frac{1}{L_{E_g}}\mathbf{I}_{d_3}\mathbf{V}_s \\
\frac{d}{dt}\mathbf{I}_c &= \frac{R_s}{L_c}\mathbf{I}_{d_3}\mathbf{I}_g + \left(-\frac{R_{E_c}}{L_c}\mathbf{I}_{d_3} - \mathbf{D}_3\right)\mathbf{I}_c \\
&\quad + \frac{1}{L_c}\mathbf{I}_{d_3}\mathbf{V}_f - \frac{[\mathbf{G}]}{L_c}\mathbf{V}_{\mathrm{dc}} \\
\frac{d}{dt}\mathbf{V}_f &= \frac{1}{C_f}\mathbf{I}_{d_3}\mathbf{I}_g - \frac{1}{C_f}\mathbf{I}_{d_3}\mathbf{I}_c - \mathbf{D}_3\mathbf{V}_f \\
\frac{d}{dt}\mathbf{V}_{\mathrm{dc}} &= \frac{\boldsymbol{\gamma}}{C_{\mathrm{dc}}}\mathbf{I}_c + \left(-\frac{1}{R_L\, C_{\mathrm{dc}}}\mathbf{I}_d - \mathbf{D}\right)\mathbf{V}_{\mathrm{dc}} + \frac{1}{C_{\mathrm{dc}}}\mathbf{I}_d\mathbf{I}_s
\end{aligned} \tag{20}$$

where $\mathbf{I}_g = [\mathbf{I}_{ga}, \mathbf{I}_{gb}, \mathbf{I}_{gc}]^T$, $\mathbf{I}_c = [\mathbf{I}_{ca}, \mathbf{I}_{cb}, \mathbf{I}_{cc}]^T$, and $\mathbf{I}_s$ are mapping the EHD variables from the time-domain grid current $\mathbf{i}_g$, converter current $\mathbf{i}_c$, and dc current source i_s, respectively. Similarly $\mathbf{V}_f = [\mathbf{V}_{fa}, \mathbf{V}_{fb}, \mathbf{V}_{fc}]^T$, $\mathbf{V}_s = [\mathbf{V}_{sa}, \mathbf{V}_{sb}, \mathbf{V}_{sc}]^T$, and $\mathbf{V}_{\mathrm{dc}}$ are the EHD variables mapped from the time-domain voltages $\mathbf{v}_f$, $\mathbf{v}_s$, and v_{dc}, respectively. The time-domain switching signals $\mathbf{s}$ and $\mathbf{g}$ are mapped as the matrices arranges

$$[\mathbf{S}] = \begin{bmatrix} [\mathbf{S}_a] \\ [\mathbf{S}_b] \\ [\mathbf{S}_c] \end{bmatrix} \quad \text{and} \quad [\mathbf{G}] = \begin{bmatrix} [\mathbf{G}_a] \\ [\mathbf{G}_b] \\ [\mathbf{G}_c] \end{bmatrix}, \tag{21}$$

respectively, and they are formed with the harmonic content of their time domain counterparts. The coupling term is defined as $\boldsymbol{\gamma} = [\mathbf{S}_a]\mathbf{I_a} + [\mathbf{S}_b]\mathbf{I_b} + [\mathbf{S}_c]\mathbf{I_c}$.

Each EHD variable is a vector formed the complex Fourier coefficients of its corresponding time-domain variable. The size of each EHD variable, and the overall order of the EHD model is determined by the maximum fundamental frequency harmonic considered to form the EHD variables, defined as h. The EHD model, as expressed in (20), is a generic model which is valid for any modulation technique or employed switching method. Although similar in structure, particular EHD models are obtained for each case since the switching matrices $[\mathbf{S}]$ and $[\mathbf{G}]$ are formed with the particular harmonic content of their corresponding time-domain switching signals. Notice that if those are not periodic, the resultant switching matrices are time varying. However for sinusoidal PWM-based modulation techniques with fixed modulation variables, e.g., m_a, θ, and m_f, the harmonic content of the EHD switching matrices is constant. Under these assumptions, the EHD system model (20) is an LTI representation of the case study system which explicitly contains all the harmonic relationships among their electrical variables derived from the used modulation technique.

In this way, the derivation and further implementation of the EHD model (20) relies on an efficient way to calculate its switching matrices. For sinusoidal PWM modulation techniques, the harmonic content of the time-domain switching signals can be

calculated with common methods such as FFT methods [22] and/or double Fourier series analysis [32]. As a part of the proposed EHD modeling methodology, an alternative to derive the harmonic content of the switching signals is proposed. This is based on the time domain formulation of the switching signal (18) which explicitly considers the characteristics of the modulation signal as described in (19).

A. Modeling of PWM Techniques in the EHD

The consideration of specific modulation techniques on the EHD models is obtained by considering the harmonic content of the time-domain switching signals into their switching matrices. For any periodic time-domain switching function, the complex series Fourier formula in (1) can be used to calculate its harmonic content. Since the switching signals only hold values of zero or one, their behavior is can be stated by the time instants when their value toggle, where the nth switching instant is denoted as $(t_{x(n)})$, with $x = (a, b, c)$. In this way, the kth complex Fourier coefficient of a time-domain switching signal is given by

$$S_{x\langle k\rangle} = \begin{cases} -\dfrac{1}{j\pi k}\displaystyle\sum_{n=1}^{2m_f}(-1)^n e^{-j\omega_0 k t_{x(n)}} & s(0)=0 \\ -\dfrac{1}{j\pi k}\displaystyle\sum_{n=1}^{2m_f}(-1)^{n+1} e^{-j\omega_0 k t_{x(n)}} & s(0)=1. \end{cases} \tag{22}$$

Each switching instant is the time when the carrier signal $c(t)$ and the modulation signal $m_x^{\mathrm{m}}(t)$ are equal. By using the time-domain description of the modulation signal proposed in (19), an approximation formula to solve this equation for the nth switching instant is given by [33]

$$t_{x(n)}^{i+1} = \begin{cases} t_{x(n)}^{i} - \dfrac{s_x^{\mathrm{m}}|_{t_{x(n)}^i} - (-1)^{n+1} m_p (t_{x(n)}^i - a_{(n)}) + 1}{\frac{d}{dt} s_x^{\mathrm{m}}|_{t_{x(n)}^i} - (-1)^{n+1} m_p} & ; s(0)=0 \\ t_{x(n)}^{i} - \dfrac{s_x^{\mathrm{m}}|_{t_{x(n)}^i} - (-1)^{n} m_p (t_{x(n)}^i - a_{(n)}) - 1}{\frac{d}{dt} s_x^{\mathrm{m}}|_{t_{x(n)}^i} - m_p} & ; s(0)=1 \end{cases} \tag{23}$$

where i is the iteration number to calculate the solution of each switching instant, three iterations is enough to obtain an accurate solution. The guess value of the iterative solution is given by $t_{x(n)}^0 = a_{(n)}$, where $a_{(n)}$ is the nth time when the slope of the carrier signal changes and is given by $a_{(n)} = \frac{(2n-1)T_0}{4m_f}$ and m_p is the slope of the carrier signal given by $m_p = \frac{4m_f}{T_0}$ Notice that the number of switching instants to calculate is $2m_f$ and by definition $t_{x(2m_f+1)} = T_0$ and $t_{x(0)} = 0$.

In this way, (22) offers a generic, light, and easy programmable methodology to obtain the harmonic content of the switching signals. This formulation can be directly extended to consider nonideal modulation conditions, such as modulation frequencies not multiples of the fundamental frequency, dead time band, and also regular sampling. Based on this methodology, other converter topologies, along with their particular modulation schemes, can be modeled in the EHD, as long as the switching signals of their equivalent time-domain switched models are available to be described in terms of switching instants.

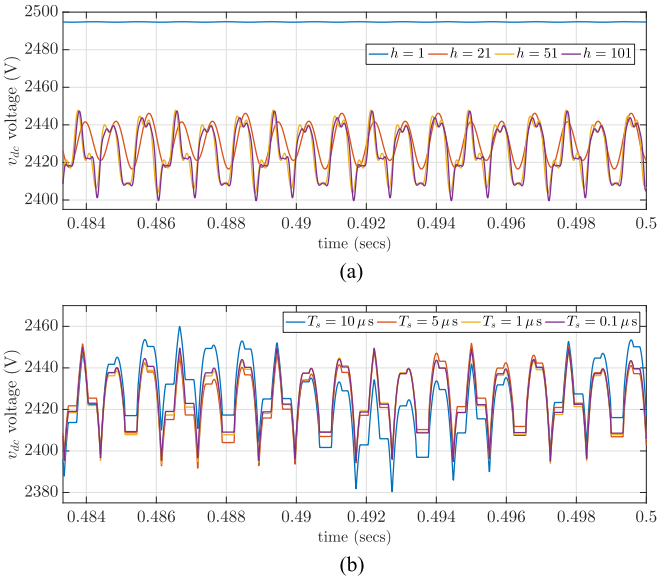

Fig. 2. v_{dc} voltage under different simulation parameters. (a) EHD solution. (b) Time-domain solution.

TABLE I
TEST SYSTEM SIMULATION PARAMETERS

Parameter	Value	Parameter	Value
L_s (mH)	1	R_s (Ω)	0.1
L_g (mH)	0.1	R_{Lg} (Ω)	0.1
L_c (mH)	1	R_{Lc} (Ω)	0
C_f (μF)	100	R_d (Ω)	0.1
C_{dc} (μF)	1000	R_L (Ω)	∞
V_s (V)	500	i_s (A)	0
f_0 (Hz)	60	m_a	0.7
m_f	15	θ (rad)	-0.2

In order to illustrate this proposal, the MATLAB functions for the calculation of the switching times and the Toeplitz switching function matrices $[\mathbf{S}_x]$ and $[\mathbf{G}_x]$, considering the three modulation techniques, are provided in the supplementary downloadable files.

B. Implementation of EHD Model

From the EHD modeling perspective, one of the key parameter is the number of considered harmonics, denoted as h. Large values of h result in highly accurate signals at the cost of very large models, which can be difficult to handle and slow to simulate. Small values of h lead to a convenient model but with low accuracy.

In order to show the impact on the selection of this parameter, Fig. 2(a) shows the simulation results of the model considering different values of h using the parameters shown in Table I. Notice that as small is the value of h less accuracy regarding the harmonic information is retained by the model. The special case of $h = 1$ is equivalent to the widely used average model, since only the fundamental frequency is considered. For this particular case, the average model simulation (EHD with h=1) shows a noticeable difference in both, the harmonic content of the signal

TABLE II
NUMBER OF DIFFERENTIAL EQUATIONS FOR SIMPLIFIED EHD MODELS

Model	$m_f = 9$ $h = 101$	$m_f = 15$ $h = 151$	$m_f = 27$ $h = 271$	$m_f = 45$ $h = 451$	$m_f = 63$ $h = 631$
EHD 3P	2030	3030	5430	9030	12630
EHD 1P	812	1212	2172	3612	5052
EHD 1P ES	237	357	637	1057	1477
EHD 1P AS	209	261	227	175	159

and the steady-state value, compared with the higher order EHD models due to the disregard of the harmonic information.

In Fig. 2(b) a simulation of the time domain model, using the trapezoidal numerical integration method, is also presented to show the numerical oscillations due to the inconsistent initial conditions introduced by the discontinuous switching functions, for different step sizes T_s. Notice that, in the EHD model the stiffness is not an issue since the switching signals are decomposed into the switching matrices as continuous signals. In order to show the straightforward implementation of the EHD model, using the proposed modeling approach along with the provided functions, MATLAB-based functions used to simulate, both the EHD model and the time domain model, are also provided in the supplementary downloadable files.

Some of the advantages that the EHD model offers are shown in Fig. 2. Notice that even for small values of h, the signals show a periodic behavior, which is not the case for time-domain simulations under large time steps. Another advantage is that an equivalent model of the average model is contained in the EHD model, which can be obtained by considering $h = 1$. Also, for fixed modulation parameters, the steady state can be obtained by solving the algebraic equation system when the dynamics are equal to zero. In fact, for this condition, the EHD model can be expressed as a linear state-space model, as expressed in (15), and allows its usage in dynamic and steady-state studies and analyses by taking advantage of this LTI structure which considers all the harmonic cross-coupling interactions. Notice that despite the size, any VSC-based system is able to be modeled by time-domain switched models for which equivalent EHD models can be derived by using the proposed methodology to obtain the harmonic content of their switching matrices from the calculation of the time-domain switching instants.

However, one of the main limitations of EHD modeling is its increased size when the maximum considered harmonic h is high. Since the switching frequency of the PWM block is the main source of harmonics it is usually of interest to consider this effect. In such case as rule of thumb a selection $h = 10m_f$ is recommended. Table II shows the order model of the three-phase model (EHD 3P) for different values of h as the modulation frequency increases. The increased order model of the obtained EHD models could derive into unfeasible implementations due to the associated long computational times, despite their advantages over the time-domain model.

V. SIMPLIFIED EHD MODELS

The following sections present the basis and assumptions that support three proposed simplifications, which in some cases are able to be combined, depending on the characteristics of the system. All of the proposed simplifications consider already constructed EHD complete models as a base on which the modulation is already included on their EHD switching matrices. This results in generic simplifications, which can be used independently on the topology or modulation technique used.

A. EHD Single Phase Model (EHD 1P)

This simplification is proposed for the balanced three-phase conditions, for which the following relationships for currents, voltage and switching functions, respectively, are satisfied:

$$I_{b\langle k\rangle} = I_{a\langle k\rangle} e^{\frac{-jk2\pi}{3}} \qquad I_{c\langle k\rangle} = I_{a\langle k\rangle} e^{\frac{-jk4\pi}{3}} \tag{24}$$

$$V_{b\langle k\rangle} = V_{a\langle k\rangle} e^{\frac{-jk2\pi}{3}} \qquad V_{c\langle k\rangle} = V_{a\langle k\rangle} e^{\frac{-jk4\pi}{3}} \tag{25}$$

$$S_{b\langle k\rangle} = S_{a\langle k\rangle} e^{\frac{-jk2\pi}{3}} \qquad S_{c\langle k\rangle} = S_{a\langle k\rangle} e^{\frac{-jk4\pi}{3}} \tag{26}$$

and therefore only one phase of each three-phase signals is enough to represent the system.

An efficient and compact implementation requires the derivation of appropriate EHD matrices. In order to illustrate this situation, consider the EHD 3P model (20). For the balanced operating conditions, the ac EHD state variables $\mathbf{I}_g$, $\mathbf{I}_c$, and $\mathbf{V}_f$ can be directly referred to one phase, since those are inherently decoupled. However, for the dc voltage EHD state variable $\mathbf{V}_{\rm dc}$ the ac EHD vectors are not explicitly decoupled. In order to propose an equivalent decoupled equation, let us define the coupling term in the dc EHD state variable as

$$[\boldsymbol{\gamma}] = [\mathbf{S}_a]\mathbf{I_a} + [\mathbf{S}_b]\mathbf{I_b} + [\mathbf{S}_c]\mathbf{I_c}. \tag{27}$$

Hence, the dc voltage EHD 1P state equation is given by

$$\frac{d}{dt}\mathbf{V}_{\rm dc} = \frac{[\boldsymbol{\Gamma}_x]}{3\,C_{\rm dc}} + \left(-\frac{1}{R_L\,C_{\rm dc}}\mathbf{I}_d - \mathbf{D}\right)\mathbf{V}_{\rm dc} + \frac{1}{C_{\rm dc}}\mathbf{I}_d\mathbf{I}_s \tag{28}$$

where $[\boldsymbol{\Gamma}_x]$ is a simplified matrix obtained from the relation $\boldsymbol{\gamma} = 3[\boldsymbol{\Gamma}_a]\mathbf{I}_a = 3[\boldsymbol{\Gamma}_b]\mathbf{I}_b = 3[\boldsymbol{\Gamma}_c]\mathbf{I}_c$, which is defined by

$$\Gamma_x^{h+1+m} = \begin{cases} S_x^{h+1+m} & \text{for} \quad m = 0, \pm 6, \pm 12, \ldots, \pm h \\ 0 & \text{for} \quad m \neq 0, \pm 6, \pm 12, \ldots, \pm h \end{cases} \tag{29}$$

with Γ_x^n as the nth row of $[\boldsymbol{\Gamma}_x]$ and S_x^n is the nth row of $[\mathbf{S}_x]$, for $x = a, b, c$.

In general, the balanced three-phase systems can always be referred to one phase by obtaining appropriate one phase relationships of the ac coupling terms in the three-phase models, such as $[\boldsymbol{\Gamma}]$ in (28). Table II shows the size model reduction for the study case model compared with the complete three-phase model (EHD 3P).

B. EHD Exact Simplified Model (EHD ES)

This simplification proposal is based on previously known harmonic pattern of the PWM modulation techniques, i.e., for m_f selected as an odd multiple of three, odd and triplen harmonic components vanish. For the dc voltage, this m_f selection results in the cancellation of all nonmultiple of six harmonics.

This harmonic cancellation allows us to simply eliminate the trivial differential equations of the zero harmonics from an

already constructed EHD 3P or EHD 1P model. The resulting simplified model will have the same structure and EHD variables as the original; but considering a reduced order size on its EHD variables, rather than the original size of $2h+1$. In this way, each EHD variable has to be accompanied by a harmonic index vector, which contains the harmonic number of each EHD variable elements, to perform analysis and reconstructions to time-domain signals. All the previously defined differentiation and multiplication operations required in order to construct the EHD model have to be reformulated to consider the index vector of each variable. As a result, a simplified model with a reduced number of differential equations is obtained. Table II shows the obtained order model for different values of h of the test system, where a dramatic reduction in the number of differential equations is obtained without compromising the accuracy of the system solution.

C. Approximate Model EHD (EHD AS)

This simplification proposal has the same elimination principle of the EHD ES and, as in this case, the resulting simplified model will have the same structure and variables as the original. The main difference is that instead of eliminating the differential equations based on the previous knowledge, a steady-state solution of the EHD 3P model or EHD 1P model is obtained with (15) to determine the state variables that have low significance into the model and eliminate them, based on certain discriminator value.

This simplification proposal can be applied to systems that do not meet the balanced conditions and/or systems where the harmonic response is not able to be predicted from the reference operating conditions.

The adequate selection of the discriminator value is essential to obtain accurate results on this simplification proposal. It is recommended to define it in terms of the fundamental harmonic of the signal under analysis. In general a discriminator value below of 1×10^{-4} p.u. maintains adequately the characteristics of the system and reduces dramatically the order of the resulting EHD model, as shown in Table II. Notice that in contrary to the previous approaches, this simplification proposal could have different order models depending on the used modulation technique. Results of Table II consider only the SPWM modulation technique since there are not significant variations compared with the others PWM techniques.

D. Comparison and Snalysis of EHD Models

In order to compare the computational effort improvement offered by the proposed simplified EHD models, a simulation-based test bench is proposed. The system used in the performed simulations for all the EHD and time-domain models is the presented in Fig. 1, considering the parameters of Table I, except the m_f value which is given in Table III for each case. In this way, the required time to perform a simulation of 0.5 s for the different proposed EHD models is used as performance parameter. In addition, the simulation time for the time-domain switched model in (16) is included to compare the proposed simplifications against this well established model. For the EHD models, the simulations are performed using MATLAB ODE 45 built-in solver using default options considering a maximum harmonic $h=10*mf+1$. For the time-domain models the ODE15s built-in solver with default options was used since this algorithm offers good simulation results for stiff models. Since the simulations for the EHD 3P and EHD 1P models with large values of h require prohibitive computation times, those are estimated using the available information. The results of this analysis are given in Table III.

TABLE III
SIMULATION TIME IN SECONDS OF THE TEST SYSTEM FOR EHD AND TIME-DOMAIN MODELS

Model	Technique	$m_f=9$	$m_f=15$	$m_f=27$	$m_f=45$	$m_f=63$
EHD 3P	SPWM	845	5783	53389*	370310*	1324600*
	THPWM	850.4	5812	53684*	372480*	1335900*
	SVPWM	853.8	6312	63503*	474860*	1789300*
EHD 1P	SPWM	100.3	368.2	3992.3	23404	75642*
	THPWM	99.4	360.8	2411.1	23414	103840*
	SVPWM	96.8	358.2	2400.2	23345	103420*
EHD 1P ES	SPWM	12.6	20.9	176.6	2094	6630
	THPWM	9.7	21.6	117.4	2471	10578
	SVPWM	9.4	21	115.8	2300	10221
EHD 1P AS	SPWM	10.5	17.64	24.7	36	52.7
	THPWM	9.2	16	24.7	43.6	57.3
	SVPWM	8.9	16.5	33.2	58.1	80
T-D sw**	SPWM	17.6	31.8	45.3	74.0	89.3
	THPWM	16.9	31.2	42.1	63.3	86.9
	SVPWM	51.7	63.0	90.1	136.8	189.6

*obtained by curve fitting **Time-domain switching model

As shown in Table III, the EHD 1P AS is the fastest model and its performance is comparable in simulation time with the time-domain switched model. Although the main intention of EHD models is not focused on simulation, these results give an insight of the level of simplification obtained with the EHD simplified proposals. The benefits of the EHD AS model were previously demonstrated by the size of their models as shown in Table II. The size represents less than 1.3% of the conventional EHD model (EHD 3P) for the case when $h=631$. In this case, the simulation time of the EHD 1P AS model is improved around 100 and 22 000 times compared with the conventional EHD 3P model, for the smallest and largest value of h, respectively.

In respect to the model accuracy, it is important to point out that the EHD 3P, EHD 1P, and EHD 1P ES models have exactly the same response without any loss of information, and for $h>10m_f$, these solutions practically overlap with the time-domain model solution. For the EHD 1P AS model, there is some loss of information due to the neglected harmonics; however, this is negligible compared with the extremely reduced order gained. The presented case has an average normalized mean square error of 4.782×10^{-4} on the EHD 1P AS model solution against the EHD 3P solution.

If used properly, the EHD AS model offers the best tradeoff between size and accuracy compared with previous proposals, although it requires additional computational effort to calculate the EHD steady state. The EHD ES model is best suited for cases with well-known switching operating conditions and its implementation does not require any further calculations, however its size is bigger than the EHD 1P AS. If it is required to

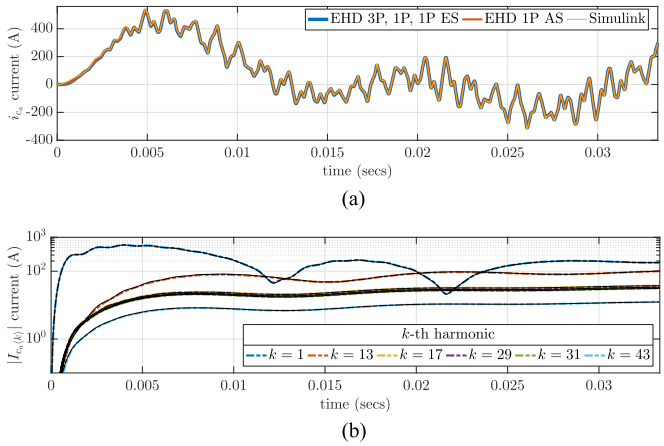

Fig. 3. Validation of dynamic response of EHD models. (a) Comparison against time-domain simulation. (b) Harmonic evolution.

analyze the phase unbalances, the EHD 1P AS and ES are not an option and the EHD 3P ES or AS should be used.

VI. EHD Models Evaluation

A. EHD Models: Dynamic Evolution

The dynamic responses of all the derived EHD models are evaluated and compared against a switched model implemented in Simulink SimPowerSystems. For this purpose consider the system of Fig. 1 with the parameters of Table I. Fig. 3(a) shows the time-domain transient response comparison converter current i_{c_a} between the EHD models simulation, with $h = 150$, and the simulink model simulation with $T_s = 1 \times -10^{-7}$ s. All the simulations consider the initial conditions equal to zero for the time-domain and EHD state variables. Notice that EHD 3P, EHD 1P, and EHD 1P ES models are exactly equal in their response for which only one waveform is used to represent them. Fig. 3(b) shows the dynamic evolution for the most relevant converter current harmonics. Notice that dynamics of individual harmonics is the natural response of the EHD models, their reconstruction into time domain-signals, such as presented in Fig. 3(a), require additional processing by using the complex Fourier formula given in (1).

From Fig. 3 it can be seen that all the EHD models have accurate dynamic responses compared with the time-domain switched model. This validates their performance under dynamic conditions.

B. EHD Models: Experimental Validation

An experimental setup is used to validate the steady state of the proposed EHD models and this considers the circuit given in Fig. 1 with the parameters of Table IV using the SPWM technique. The response is compared with the simulation result of the EHD 1P AS model with the same parameters, considering $h = 210$ and a discriminator value of 1×10^{-4} pu. The EHD 1P AS model is used to validate all the EHD model proposals since, as explained previously, the difference between them is negligible for the selected discriminator value.

TABLE IV
Parameters for Experimental Validation

Parameter	Value	Parameter	Value
f_0 (Hz)	60	V_s (V)	33.26
$C_{\rm dc}$ (μF)	922	i_s (A)	0
R_s (Ω)	1.75	L_s (mH)	0.44
$R_{L\,(\Omega)}$	112.3	m_a	0.8020
m_f	21	θ (rad)	-0.18
L_g (mH)	6.3	R_{Lg} (Ω)	1.57
L_c (mH)	11.3	R_{Lc} (Ω)	2.51
C_f (μF)	33	R_d (Ω)	3.78

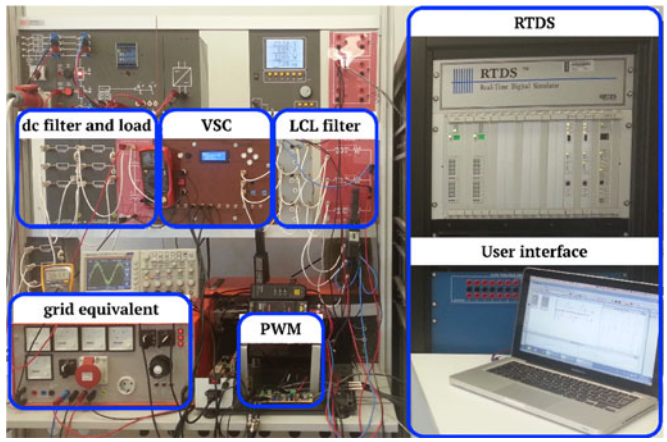

Fig. 4. Experimental setup.

The experimental setup considers an open-loop control strategy with fixed modulation parameters, i.e., amplitude m_a and phase angle θ, referred to the point of common coupling. The phase synchronicity is obtained by means of a phase-locked-loop implemented on a real time digital simulator (RTDS) along with the user interface to set the modulation parameters. The modulation signals generated in the RTDS are the inputs to the analogue PWM. Fig. 4 shows the general layout of the experimental setup.

The EHD 1P AS model, referred to phase a, of the experimental setup is given by

$$\begin{aligned}
\frac{d}{dt}\mathbf{I}_{g_a} &= \left(-\frac{R_{E_g}}{L_{E_g}}\mathbf{I}_d - \mathbf{D}\right)\mathbf{I}_{g_a} + \frac{R_d}{L_{E_g}}\mathbf{I}_d\mathbf{I}_{c_a} - \frac{1}{L_{E_g}}\mathbf{I}_d\mathbf{V}_{f_a} \\
&\quad + \frac{1}{L_{E_g}}\mathbf{I}_d\mathbf{V}_{s_a} \\
\frac{d}{dt}\mathbf{I}_{c_a} &= \frac{R_s}{L_c}\mathbf{I}_d\mathbf{I}_{g_a} + \left(-\frac{R_{E_c}}{L_c}\mathbf{I}_d - \mathbf{D}\right)\mathbf{I}_{c_a} + \frac{1}{L_c}\mathbf{I}_d\mathbf{V}_{f_a} \\
&\quad - \frac{[\mathbf{G}_a]}{L_c}\mathbf{V}_{\rm dc} \\
\frac{d}{dt}\mathbf{V}_{f_a} &= \frac{1}{C_f}\mathbf{I}_d\mathbf{I}_{g_a} - \frac{1}{C_f}\mathbf{I}_d\mathbf{I}_{c_a} - \mathbf{D}\mathbf{V}_{f_a} \\
\frac{d}{dt}\mathbf{V}_{\rm dc} &= \frac{3[\mathbf{\Gamma}_a]}{C_{\rm dc}}\mathbf{I}_{c_a} + \left(-\frac{1}{R_L\,C_{\rm dc}}\mathbf{I}_d - \mathbf{D}\right)\mathbf{V}_{\rm dc} + \frac{1}{C_{\rm dc}}\mathbf{I}_d\mathbf{I}_s.
\end{aligned} \tag{30}$$

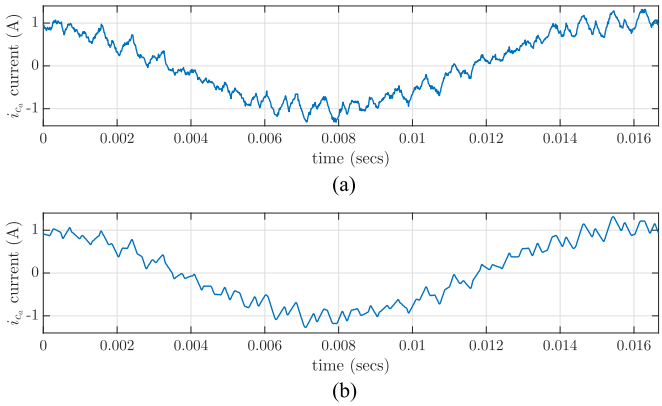

Fig. 5. Simulated and experimental i_g current signals for Fig. 1 system. (a) Measurement. (b) EHD solution.

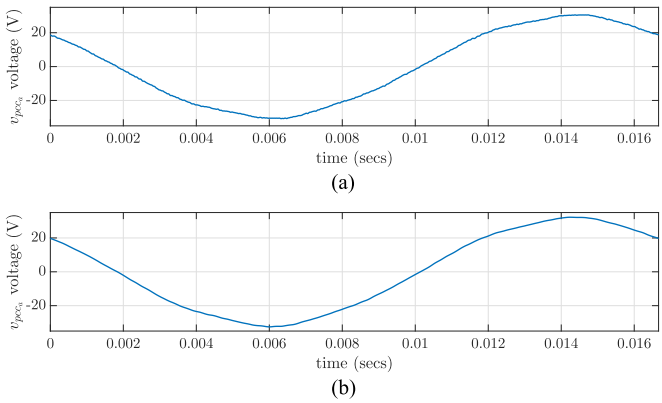

Fig. 6. Steady-state waveforms of the pcc voltage for Fig. 1 system. (a) Measured waveform. (b) EHD solution.

Figs. 5 and 6 show the comparison of the measured waveforms against the EHD solution, for the i_{g_a} current and the phase a voltage at PCC, respectively.

Figs. 5 and 6 show a high level of agreement between the EHD model solution and the real system performance. These results show that the harmonic effects produced by the nonlinear switching process are effectively retained by the simplified EHD model.

A comparison of the harmonic content for the simulated and experimental signals are presented in Fig. 7. It can be seen how the EHD model retains most of the harmonic information regarding the switching process, compared with the harmonic content of the experimental waveform. The differences between the simulations and experiments are the result of the deviations of the real operation for the VSC from the assumed modeling conditions, like the Thevenin grid equivalent, balanced operation, linear and lumped passive components, ideal switches, ideal switching process, among others. Despite the small differences, the overall level of attachment of the EHD model is in general terms excellent since it closely retains the information of the dominant harmonics in a continuous time-invariant fashion model. Hence, detailed and accurate analysis and simulations can be performed over the real system since all the relationships

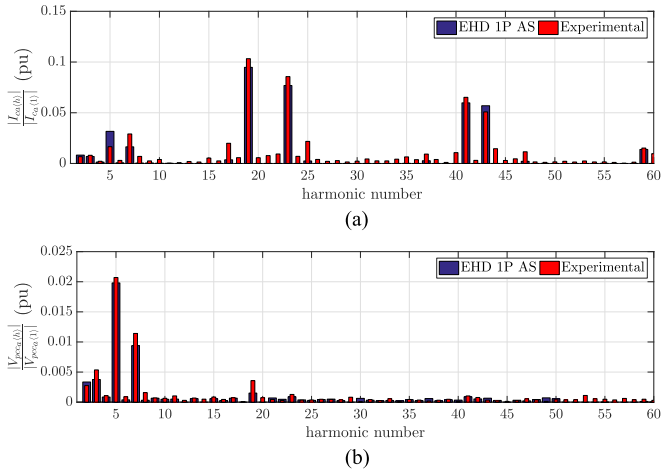

Fig. 7. Simulated and experimental harmonic content signals comparison: i_{ca} (a) and v_{pcc} (b).

of the dominant harmonics are considered in an reduced order model with an LTI fashion.

C. Discussion of the Results

The EHD model is an accurate state-space fashion model, which under certain conditions presents an LTI form. This model has the characteristic of explicitly considering each harmonic of the time domain variables as an individual state variable. As shown by the validations, it can be very accurate to represent the physical system in both, steady-state and dynamic conditions.

The average modeling has been so far enough to carry out many of the regular design and analysis tasks in power electronic systems. However, the increasingly growing necessity of explicitly considering the effects of the switching process in the models of power electronic converters, calls for the consideration of harmonic-based models, such as the proposed EHD model.

Despite the methodology and simplification provided in this work, the EHD models are still a little more complex and their derivation and handling require more effort than the averaged models. In this sense its usage should be justified by the necessity to analyze the harmonic phenomena not able to be captured by the average modeling, such as fast computation of the steady-state solution, optimal component design, parameters estimation, and harmonic stability, among others. Notice that the provided EHD modeling methodology results in a large signal model, which under certain considerations can be behave as an LTI model. From this modeling approach, further EHD small signal derivations are able to be proposed, in order to address linear analysis of well-known issues like harmonic stability problems caused by dynamic harmonic interaction between multiple closed-loop power converters.

VII. Conclusion

This paper has presented a structured methodology for the modeling of VSC-based power electronic systems in the EHD.

This contribution is based on the calculation of the switching instants, and therefore, reliable, and efficient explicit formulas were proposed for three different PWM techniques, i.e., SPWM, THPWM, and SVPWM. As an example, a grid-connected three-phase VSC-based system with an ac LCL-filter was modeled both in the time-domain and in the EHD, to show the straightforward relationship between both modeling frameworks, and the advantages offered by the EHD over the time-domain model.

Three simplified modeling approaches were proposed to deal with the increased size of the conventional EHD models. A comparison among them has been performed using a simulation-based test bench on which the benefits, in terms of computational effort, model size, and accuracy were shown. The results have revealed a size reduction of the proposed simplified modeling approaches up to 98.7% respect to the conventional EHD. Consequently, the simulation times of the proposed simplifications are up to 22 000 times faster than the conventional EHD. Besides, one of the proposed EHD modeling approaches has come to a swifter simulation time than the time-domain switched model.

Experimental validations of the most simplified model (EHD 1P AS) were carried out in which its high level of accuracy was clearly demonstrated through the waveforms and spectrum comparisons.

REFERENCES

[1] P. W. Lehn, "Exact modeling of the voltage source converter," *IEEE Trans. Power Del.*, vol. 17, no. 1, pp. 217–222, Jan. 2002.

[2] A. Houari, H. Renaudineau, J.-P. Martin, B. Nahid-Mobarakeh, S. Pierfederici, and F. Meibody-Tabar, "Large-signal stabilization of ac grid supplying voltage-source converters with LCL-filters," *IEEE Trans. Ind. Appl.*, vol. 51, no. 1, pp. 702–711, Jan. 2015.

[3] M. Esparza and J. Segundo-Ramírez, "An exact method for analysis and component design of grid connected VSC-based power devices," *Int. J. Electr. Power Energy Syst.*, vol. 78, pp. 489–498, Jun. 2016.

[4] J. Segundo-Ramírez, A. Medina, A. Ghosh, and G. Ledwich, "Stability boundary analysis of the dynamic voltage restorer in weak systems with dynamic loads," *Int. J. Circuit Theory Appl.*, vol. 40, no. 6, pp. 551–569, Jun. 2012.

[5] C. Wan, M. Huang, C. Tse, and X. Ruan, "Effects of interaction of power converters coupled via power grid: A design-oriented study," *IEEE Trans. Power Electron.*, vol. 30, no. 7, pp. 3589–3600, Jul. 2015.

[6] X. Wang, F. Blaabjerg, and P. C. Loh, "Virtual RC damping of LCL-Filtered voltage source converters with extended selective harmonic compensation," *IEEE Trans. Power Electron.*, vol. 30, no. 9, pp. 4726–4737, Sep. 2015.

[7] X. Wang, F. Blaabjerg, M. Liserre, Z. Chen, J. He, and Y. Li, "An active damper for stabilizing power-electronics-based AC systems," *IEEE Trans. Power Electron.*, vol. 29, no. 7, pp. 3318–3329, Jul. 2014.

[8] G. Agundis-Tinajero *et al.*, "Harmonic issues assessment on PWM VSC-based controlled microgrids using Newton methods," *IEEE Trans. Smart Grid*, vol. PP, no. 99, pp. 1–1, 2016.

[9] D. Liberzon, *Switching in Systems and Control*. New York, NY, USA: Springer, 2012.

[10] D. Maksimovic, A. M. Stankovic, V. J. Thottuvelil, and G. C. Verghese, "Modeling and simulation of power electronic converters," *Proc. IEEE*, vol. 89, no. 6, pp. 898–912, Jun. 2001.

[11] M. Lindgren, "Modeling and control of voltage source converters connected to the grid," Ph.D. dissertation, Chalmers Univ. Technol., Göteborg, Sweden, 1998.

[12] X. Wang, F. Blaabjerg, and W. Wu, "Modeling and analysis of harmonic stability in an AC power-electronics-based power system," *IEEE Trans. Power Electron.*, vol. 29, no. 12, pp. 6421–6432, Dec. 2014.

[13] X. Wang, Y. Li, F. Blaabjerg, and P. Loh, "Virtual-impedance-based control for voltage-source and current-source converters," *IEEE Trans. Power Electron.*, vol. 30, no. 12, pp. 7019–7037, Dec. 2015.

[14] A. Reznik, M. Simoes, A. Al-Durra, and S. Muyeen, "Filter design and performance analysis for grid-interconnected systems," *IEEE Trans. Ind. Appl.*, vol. 50, no. 2, pp. 1225–1232, Mar. 2014.

[15] D. Infield, P. Onions, A. Simmons, and G. Smith, "Power quality from multiple grid-connected single-phase inverters," *IEEE Trans. Power Del.*, vol. 19, no. 4, pp. 1983–1989, Oct. 2004.

[16] R. N. Beres, X. Wang, F. Blaabjerg, M. Liserre, and C. L. Bak, "Optimal design of high-order passive-damped filters for grid-connected applications," *IEEE Trans. Power Electron.*, vol. 31, no. 3, pp. 2083–2098, Mar. 2016.

[17] A. Albanna and C. Hatziadoniu, "Harmonic modeling of hysteresis inverters in frequency domain," *IEEE Trans. Power Electron.*, vol. 25, no. 5, pp. 1110–1114, May 2010.

[18] T. H. Demiray, "Simulation of power system dynamics using dynamic phasor models," Ph.D. dissertation, EEH—Power Systems Laboratory, Zurich, Switzerland, 2008.

[19] J. Segundo-Ramirez, E. Barcenas, A. Medina, and V. Cardenas, "Steady-state and dynamic state-space model for fast and efficient solution and stability assessment of ASDs," *IEEE Trans. Ind. Electron.*, vol. 58, no. 7, pp. 2836–2847, Jul. 2011.

[20] A. Medina *et al.*, "Harmonic analysis in frequency and time domain," *IEEE Trans. Power Del.*, vol. 28, no. 3, pp. 1813–1821, Jul. 2013.

[21] J. Rico, M. Madrigal, and E. Acha, "Dynamic harmonic evolution using the extended harmonic domain," *IEEE Trans. Power Del.*, vol. 18, no. 2, pp. 587–594, Apr. 2003.

[22] G. Love and A. Wood, "Harmonic state space model of power electronics," in *Proc. 2008 13th Int. Conf. Harmonics Quality Power*, Sep. 2008, pp. 1–6.

[23] H. Garcia, M. Madrigal, B. Vyakaranam, R. Rarick, and F. E. Villaseca, "Dynamic companion harmonic circuit models for analysis of power systems with embedded power electronics devices," *Electr. Power Syst. Res.*, vol. 81, no. 2, pp. 340–346, Feb. 2011.

[24] J. Kwon, X. Wang, C. Bak, and F. Blaabjerg, "The modeling and harmonic coupling analysis of multiple-parallel connected inverter using harmonic state space (HSS)," in *Proc. 2015 IEEE Energy Convers. Cong. Expo.*, Sep. 2015, pp. 6231–6238.

[25] J. Kwon, X. Wang, C. Bak, and F. Blaabjerg, "Harmonic interaction analysis in grid connected converter using harmonic state space (HSS) modeling," in *Proc. 2015 IEEE Appl. Power Electron. Conf. Expo.*, Mar. 2015, pp. 1779–1786.

[26] J. Orillaza, M. Hwang, and A. Wood, "Switching instant variation in harmonic state-space modelling of power electronic devices," in *Proc. 2010 20th Australasian Universities Power Eng. Conf.*, Dec. 2010, pp. 1–5.

[27] M. Esparza and J. Segundo-Ramírez, "Optimal design of power electronics converters using the extended harmonic domain," in *Proc. 2014 IEEE Int. Autumn Meet. Power, Electron. Computing.*, Nov. 2014, pp. 1–6.

[28] M. Esparza, J. Segundo-Ramirez, C. Nunez, X. Wang, and F. Blaabjerg, "A comprehensive design approach of power electronic-based distributed generation units focused on power quality improvement," *IEEE Trans. Power Del.*, vol. PP, no. 99, pp. 1–1, 2016.

[29] J. E. Ormrod, "Harmonic state space modelling of voltage source converters," Master Thesis, Univ. Canterbury, Christchurch, New Zealand, 2013.

[30] J. Arrillaga, A. Medina, M. L. V. Lisboa, M. A. Cavia, and P. Sanchez, "The harmonic domain: A frame of reference for power system harmonic analysis," *IEEE Trans. Power Syst.*, vol. 10, no. 1, pp. 433–440, Feb. 1995.

[31] K. Zhou and D. Wang, "Relationship between space-vector modulation and three-phase carrier-based PWM: A comprehensive analysis [three-phase inverters]," *IEEE Trans. Ind. Electron.*, vol. 49, no. 1, pp. 186–196, Feb. 2002.

[32] G. R. Ainslie-Malik, "Mathematical analysis of PWM processes," Ph.D. dissertation, Univ. Nottingham, Nottingham, U.K., 2013.

[33] J. Segundo-Ramirez, R. Peña-Gallardo, A. Medina, C. Nuñez-Gutiérrez, and N. Visairo-Cruz, "A comprehensive modeling of a three-phase voltage source PWM converter," *Math. Problems Eng.*, vol. 2015, Jul. 2015, Art. no. e426245. [Online]. Available: http://www.hindawi.com/journals/mpe/2015/426245/abs/

Authors' photographs and biographies not available at the time of publication.